Journal of Electron Spectroscopy and Related Phenomena 185 (2012) 18–22

Contents lists available at SciVerse ScienceDirect

Journal of Electron Spectroscopy and Related Phenomena

journal homepage: www.elsevier.com/locate/elspec

Electronic and optical properties of hafnium indium zinc oxide thin film by XPS and REELS

Yus Rama Denny[a], Hye Chung Shin[a], Soonjoo Seo[a], Suhk Kun Oh[a], Hee Jae Kang[a,*], Dahlang Tahir[b], Sung Heo[c], Jae Gwan Chung[c], Jae Cheol Lee[c], Sven Tougaard[d]

[a] Department of Physics, Chungbuk National University, Cheongju 361-763, Republic of Korea
[b] Department of Physics, Hasanuddin University, Makassar 90245, Indonesia
[c] Analytical Engineering Center, Samsung Advanced Institute of Technology, Suwon 440-600, Republic of Korea
[d] Department of Physics and Chemistry, University of Southern Denmark, DK-5230 Odense M., Denmark

ARTICLE INFO

Article history:
Received 25 August 2011
Received in revised form 8 December 2011
Accepted 12 December 2011
Available online 29 December 2011

Keywords:
REELS
XPS
HIZO
Electrical properties
Optical properties

ABSTRACT

The electronic and optical properties of GaInZnO (GIZO), HfInZnO (HIZO) and InZnO (IZO) thin films on glass substrates were investigated using X-ray photoelectron spectroscopy (XPS) and reflection electron energy loss spectroscopy (REELS). XPS results show that HIZO, GIZO, and IZO thin films have mixed metal and oxide phases. REELS spectra reveal that the band gaps of GIZO, HIZO, and IZO thin films are 3.1 eV, 3.5 eV, and 3.0 eV, respectively. These band gaps are consistent with optical band gaps determined by UV-Spectrometer. The optical properties represented by the dielectric function ε, the refractive index n, the extinction coefficient k, and the transmission coefficient T of the GIZO, HIZO and IZO thin films were determined from a quantitative analysis of REELS spectra. The transmission coefficient was increased by 4% for the HIZO compound incorporating Hf into IZO, but decreased by 3% for the GIZO compound incorporating Ga into IZO in the visible region in comparison to that of IZO.

1. Introduction

Transparent oxides such as ZnO, InZnO and GaInZnO have been attracting a great deal of attention for channel materials in applications for transparent thin film transistors (TFTs), transparent electrode in solar cells, and flat panel displays [1–6]. Amorphous gallium indium zinc oxide (a-GIZO) has been particularly a promising material because of the high mobility and a reasonably high on/off ratio in a TFT [1,3]. However, the use of GIZO in a TFT operation is limited because the threshold voltage gradually shifts under long-term bias stresses in an a-GIZO TFT [7].

To address the deterioration problem, Kim et al. fabricated TFTs using hafnium indium zinc oxide (HIZO) as the active channel. Their results suggested that Hf ions in HIZO TFTs may have an effect on improving the bias-induced instability [8]. They concluded that the InZnO compound can be used as a robust deterioration-free channel layer in TFTs by replacing Ga with Hf. The hafnium (Hf) content in a HIZO device may change the crystal structure and thereby reduce the device instability. However, the role of Hf cation in the HIZO compound was not clearly explained. While the electrical properties of HIZO were previously reported, the electronic and optical properties of HIZO remain to be unknown. Hence, it is important to understand the electronic and optical properties of HIZO thin films to establish a link between the fundamental properties of the films and the electrical properties of HIZO-based transparent TFTs.

In this paper, we used both XPS and REELS to determine the electronic properties and the optical properties of GIZO, HIZO, and IZO thin films. The band gap of an oxide thin film can be measured using REELS spectra. A quantitative analysis of REELS in conjunction with Tougaard algorithm then gives us direct information about the optical parameters of the materials using the dielectric function [9,10].

2. Experimental

GIZO, HIZO and IZO thin films were deposited on glass substrates at room temperature by RF magnetron sputtering with the RF power of 200 W in Ar gas ambience with 1% of oxygen. The sputter target composition ratio of Ga:In:Zn in GIZO, Hf:In:Zn in HIZO, and In:Zn in IZO were 33:33:33, 10:35:55, and 45:55, respectively. The physical thickness of the thin films was 40 nm. XPS measurements were performed using Mg source with the pass energy of 20 eV. The incident and take-off angles of electrons were 55° and 0° from the surface normal, respectively. The binding energies were referenced to C 1s peak of hydrocarbon contamination at 285 eV [11]. The REELS spectra were measured with the primary electron

* Corresponding author.
E-mail address: hjkang@cbu.ac.kr (H.J. Kang).

0368-2048/$ – see front matter © 2011 Elsevier B.V. All rights reserved.
doi:10.1016/j.elspec.2011.12.004

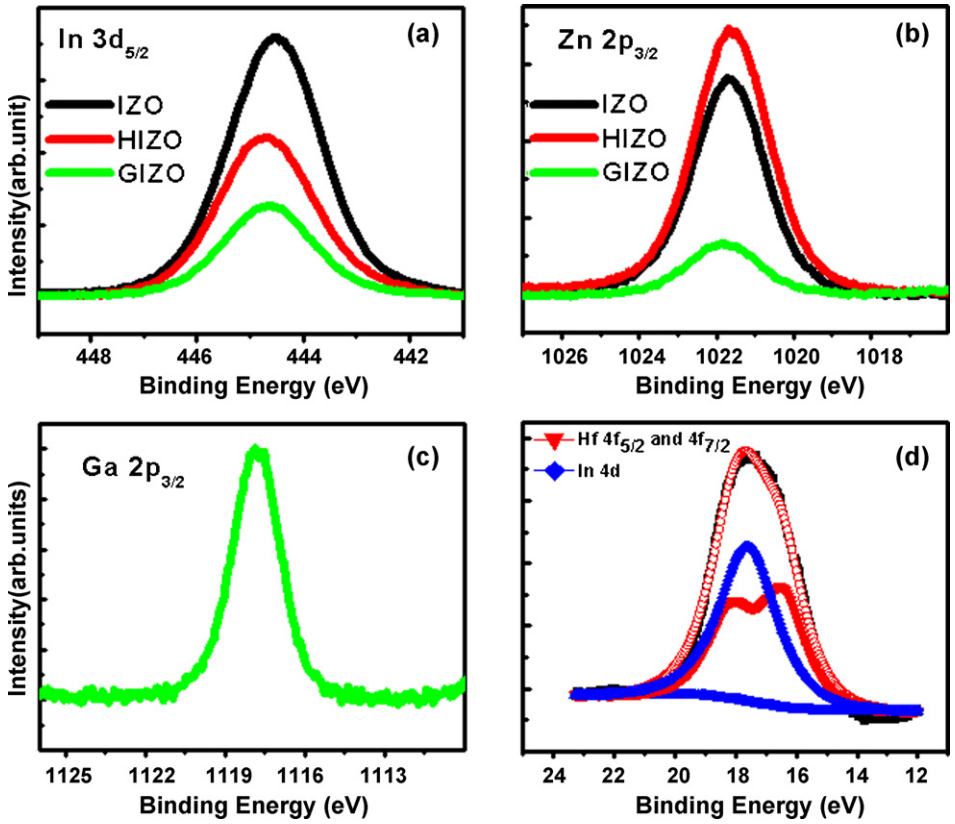

Fig. 1. XPS spectra of (a) In 3d, (b) Zn 2p, (c) Ga 2p, and (d) Hf 4f for GIZO, HIZO and IZO thin films.

energy of 1.0 and 1.5 keV for excitation and with the constant analyzer pass energy of 20 eV. The full width at half maximum (FWHM) of the elastic peak was 0.8 eV.

3. Results and discussions

Fig. 1(a) shows the In $3d_{5/2}$ photoelectron spectra obtained from GIZO, HIZO, and IZO thin films, respectively. The binding energy of In $3d_{5/2}$ at 444.5 eV corresponds to the bonding of In and O, which appeared in all of the thin films [12]. Fig. 1(b) shows the Zn $2p_{3/2}$ photoelectron spectra obtained from GIZO, HIZO, and IZO thin films. The binding energy of Zn $2p_{3/2}$ at 1021.7 eV found in all the thin films corresponds to that of the Zn—O bond [12]. Fig. 1(c) shows the Ga $2p_{3/2}$ photoelectron spectrum obtained from the GIZO thin film. The binding energy for Ga $2p_{3/2}$ is 1117.8 eV, which corresponds to the binding energy of the Ga—O bond [13]. The Hf 4f photoelectron spectrum obtained from the HIZO thin film duplicated In 4d photoelectron spectrum as shown in Fig. 1(d). Here the binding energies of Hf $4f_{5/2}$ and $4f_{7/2}$ spectra appeared at 18.1 and 16.4 eV, which correspond to the binding energy of the Hf—O bond [14]. These XPS results thus show that HIZO thin films and GIZO thin films have mixed metal and oxide phases. The surface composition ratios of Ga:In:Zn in GIZO, Hf:In:Zn in HIZO, and In:Zn in IZO thin films estimated from the quantitative analysis of XPS were 38:29:34, 7:19:74, and 41:59, respectively. The surface composition of HIZO is different from the target composition, but the surface compositions of GIZO and IZO are closer to those of the target compositions.

The REELS spectra of GIZO, HIZO and IZO thin films are shown in Fig. 2(a). The energy band gap can be determined from the REELS spectra. The plasmon loss peaks exhibiting broad peaks with the energy away from the elastic peak at 0 eV appear below the electron–hole inter-band transition. The onset of a loss spectrum is due to electron–hole excitation. The band gap energy was estimated by drawing a linear fit line along the maximum negative slope at a point near the onset of the loss signal spectrum to the background level. The cross section of the linear fit line and the background level gives the band gap value. The band gap was determined from the mean of several measurements and the uncertainty calculated from the standard deviation was ±0.1 eV. The measured band gap of GIZO, HIZO and IZO thin films was 3.1 eV, 3.5 eV and 3.0 eV, respectively within the uncertainty of ±0.1 eV. The band gap of HIZO is larger in comparison to that of either GIZO or IZO, which implies that the addition of Hf to IZO resulted in an increase in the band gap by 0.5 eV. For comparison, the optical band gap of GIZO, HIZO and IZO thin films was obtained by using UV-Spectrometer. The optical band gaps are calculated on the basis of the optical spectral absorption and can be determined by the extrapolation of best fit line between $(\alpha h\upsilon)^2$ and $h\upsilon$ with α, h, and υ which are the absorption coefficient, the Planck's constant, and the frequency of incident photon, respectively. As shown in Fig. 2(b), the optical band gap for GIZO, HIZO and IZO thin films was 3.19, 3.50, and 3.07 eV, respectively. The optical band gaps are consistent with band gap values determined by REELS spectra.

The optical parameters of GIZO, HIZO and IZO thin films were determined via a model using Tougaard–Yubero QUEELS-ε(k,ω)-REELS software package [9,15]. In this model, the response of the material to a moving electron is represented in terms of the dielectric function ε, which is conveniently described by the energy loss function (ELF) $\mathrm{Im}(-1/\varepsilon)$. The ELF can be expressed as a sum of Drude–Lindhard type oscillators given by [16],

$$Im\left\{\frac{-1}{\varepsilon(k,\omega)}\right\} = \theta(\hbar\omega - E_g)\cdot\sum_{i=1}^{n}\frac{A_i\gamma_i\hbar\omega}{\left(\hbar^2\omega_{0ik}^2 - \hbar^2\omega^2\right)^2 + \gamma_i^2\hbar^2\omega^2} \quad (1)$$

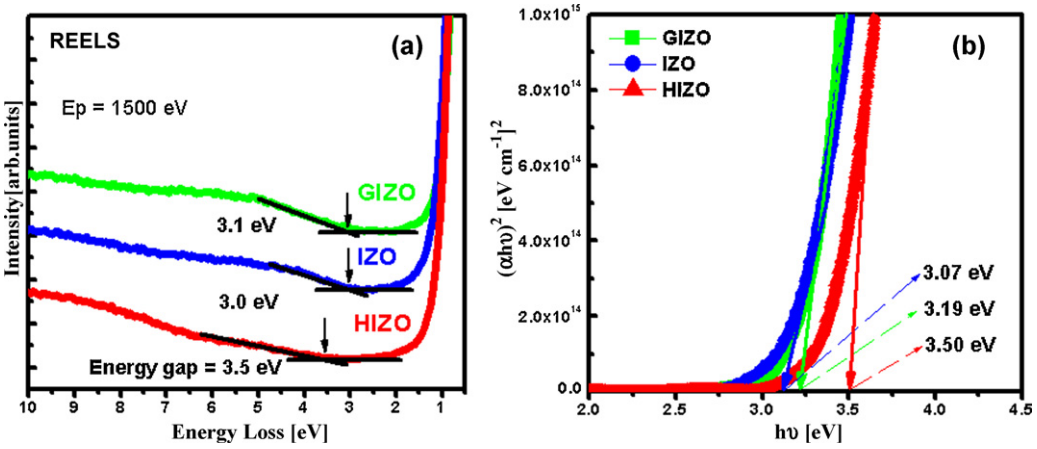

Fig. 2. (a) Reflection electron energy loss spectra with the primary energy of 1500 eV and (b) plot of $(\alpha h\upsilon)^2$ versus $h\upsilon$ for GIZO, HIZO and IZO thin films.

with the dispersion relation

$$\hbar\omega_{0ik} = \hbar\omega_{0i} + \alpha_i \frac{\hbar^2 k^2}{2m}, \tag{2}$$

where A_i, γ_i, $\hbar\omega_i$, and α_i are the oscillator strength, the damping coefficient, the excitation energy, and the momentum dispersion coefficient of the ith oscillator, respectively.

The excitation energy $\hbar\omega_i$, corresponds to the main peak of energy loss position, the oscillator strength A_i is attributed to the amplitude of energy loss, and the oscillator damping coefficient γ_i is attributed to the width of peak spectra of experimental inelastic scattering cross-section in REELS spectra. The $\hbar k$ is the momentum transferred from the REELS electron to the solid. The dependence of ω_{0ik} on k is generally unknown. Because of this, the last parameter, α_i corresponds to momentum dispersion coefficient; we made α_i as an adjustable parameter. The values of the momentum dispersion coefficients α_i are related to the effective mass of the electrons, so that $\alpha_i \approx 0$ for insulator and $\alpha_i \approx 1$ for metal. Accordingly, we found that good fits were obtained with $\alpha_i = 0.05$ for all oscillators. The step function $\theta(\hbar\omega - E_g)$ is included to simulate a possible energy band gap E_g estimated from the onset of the energy loss in the REELS spectrum in Fig. 2(a).

The experimental and theoretical inelastic scattering cross sections, K_{exp} and K_{sc}, multiplied by the inelastic mean free path λ, shown in Fig. 3. The value of λK_{exp} was obtained from the background subtraction of the REELS spectra. It was fitted with parameters of A_i, γ_i, $\hbar\omega_i$, and α_i until they are comparable to the calculated inelastic cross section at various primary electron energies. The theoretical values λK_{sc} in Fig. 3 were calculated using the QUEELS-ε(k,ω)-REELS software. The parameters of the ELF based

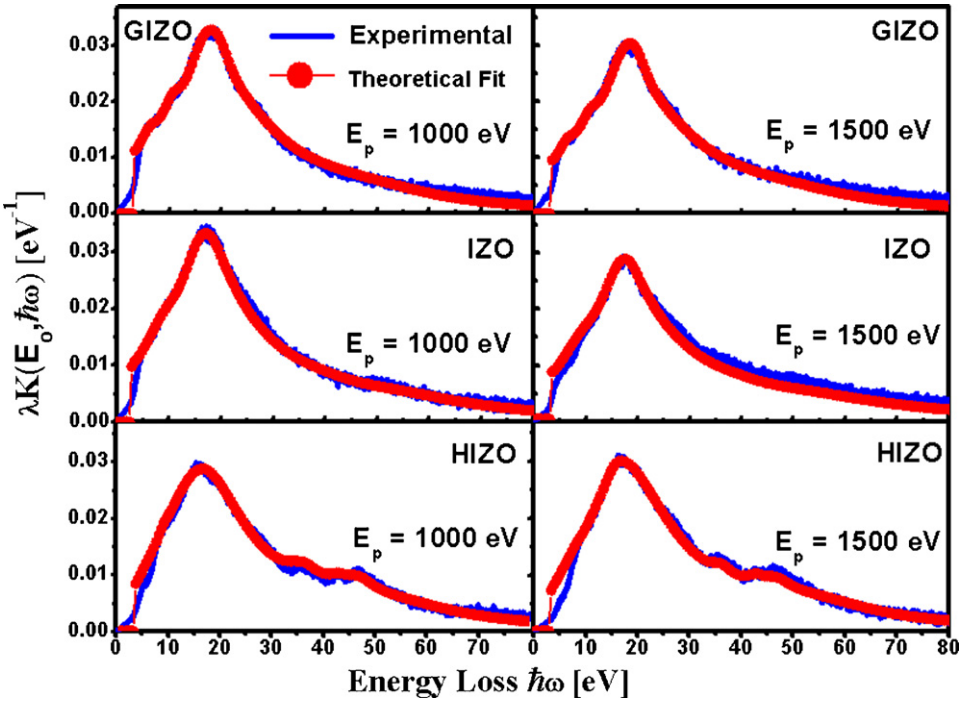

Fig. 3. Experimental inelastic cross section λK_{exp} (solid line) obtained from REELS data and the theoretical inelastic cross section λK_{th} (circle) calculated by utilizing the simulated energy loss function for primary energies of 1.0 and 1.5 keV for GIZO, HIZO and IZO thin films.

Table 1
Parameters for energy loss functions in the model of HIZO, IZO and GIZO thin films that give the best fits overall to experimental cross sections at 1.0 and 1.5 keV.

	i	$\hbar\omega_{0i}$ (eV)	A_i (eV^2)	γ_i (eV)
(HIZO)	1	8.0	0.89	4.5
(E_g = 3.5 eV)	2	16.0	5.69	5
(α_i = 0.05)	3	19.42	185.99	18
	4	26.73	100.89	25
	5	36.03	13.34	5
	6	42.61	15.56	5
	7	46.64	22.23	6
	8	55.47	133.38	25
IZO	1	11.0	10.46	10.0
(E_g = 3.0 eV)	2	18.3	101.07	8.0
(α_i = 0.05)	3	22.5	50.67	11.0
	4	28.0	135.83	19.0
	5	38.2	50.93	17.0
	6	55.0	282.18	38.0
GIZO	1	7.0	1.27	4.5
(E_g = 3.1 eV)	2	11.35	3.89	4.5
(α_i = 0.05)	3	19.4	94.13	6.5
	4	26.0	272.21	20.0
	5	40.19	132.83	29.5
	6	51.41	138.81	30.0

on Drude–Lindhard type oscillators were determined using the trial-and-error procedure until a satisfactory quantitative agreement between the experimental results and theoretical results was reached. Note that in all calculations, the same ELF was used for all energies in each GIZO, HIZO and IZO. The good agreement between the experimental and theoretical results (obtained with the same ELF) at both 1.0 and 1.5 keV gives confidence to the validity of the model and thereby in the accuracy of the determined ELF. Table 1 shows the oscillators of ELF. As shown in Table 1, the ELF for HIZO, GIZO and IZO has 8, 6 and 6 oscillators, respectively. The ELF of the HIZO thin film has 2 additional oscillators at 42.6 and 46.6 eV compared with those of the GIZO and IZO thin films. The oscillator at 46.6 eV is attributed to a contribution of Hf cations to IZO thin film and can be also found in the energy loss spectrum of HfO_2 according to another literature [17]. The strength of each oscillator is quite different. The oscillator strengths were renormalized to fulfill the Kramers–Kronig sum rule. The ELF Im$(-1/\varepsilon)$ and the surface energy loss function (SELF) Im$(-1/(1+\varepsilon))$ for GIZO, HIZO and IZO are plotted in Fig. 4 with the parameters listed in Table 1 for the energies ranging from 0 to 80 eV. The peaks of the ELFs for GIZO, HIZO and IZO are 17.4, 16.7, and 18.3 eV, respectively. Similarly, the peaks of SELF are 16.5, 13.7, and 15.5 eV, respectively. All

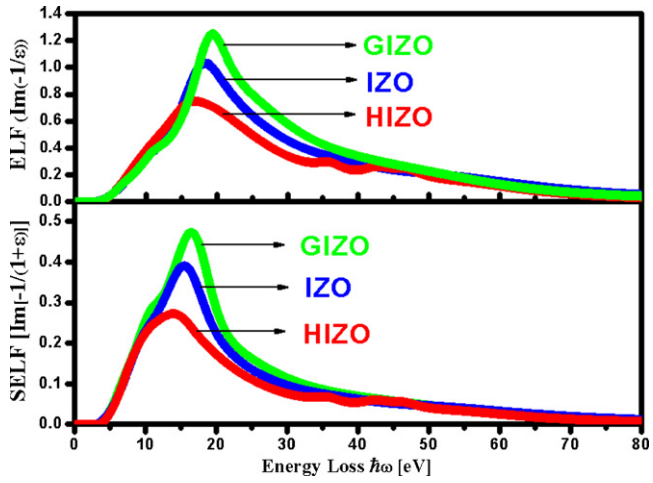

Fig. 4. Energy loss functions (ELFs) and surface energy loss function (SELF) calculated for GIZO, HIZO and IZO by utilizing the parameters given in Table 1.

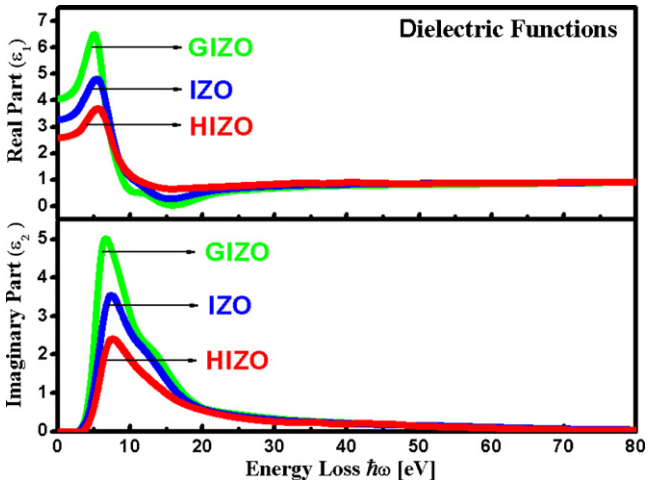

Fig. 5. Calculated data for complex dielectric function of GIZO, HIZO and IZO thin films.

the areal ratios between SELF and ELF for GIZO, HIZO and IZO are approximately 0.30. It means that about 30% of the ELF is coming from SELF. The energy loss function in Eq. (1) allows us to perform a Kramers–Kronig transformation to calculate the real part of the reciprocal of complex dielectric function. The real part ε_1 and imaginary part ε_2 can be calculated from Im$\{-1/\varepsilon\}$ and Re$\{1/\varepsilon\}$, respectively.

Fig. 5 shows the real part ε_1 and imaginary part ε_2 (corresponding to the absorption spectrum) of the dielectric functions. The main peaks of ε_1 for GIZO, IZO and HIZO fall to 5.1, 5.4, and 5.5 eV, respectively. Likewise, the main peaks of ε_2 for GIZO and IZO are 6.7, and 7.4 eV, but the peak appears at a higher value of 7.6 eV for HIZO as shown in Fig. 5. This indicates that the larger dielectric functions of HIZO resulted from Hf cation in the HIZO compound.

Refractive index n and extinction coefficient k are determined from the dielectric function by using the relations.

$$n = \sqrt{\frac{1}{2}\left(\sqrt{\varepsilon_1^2+\varepsilon_2^2}+\varepsilon_1\right)} \quad \text{and} \quad k = \sqrt{\frac{1}{2}\left(\sqrt{\varepsilon_1^2+\varepsilon_2^2}-\varepsilon_1\right)} \tag{3}$$

We determined the transmission coefficient T from the relation $R+T+\mu=1$ [16], where R is the reflection coefficient given by the relation [15]

$$R = \frac{(n-1)^2+k^2}{(n+1)^2+k^2} \tag{4}$$

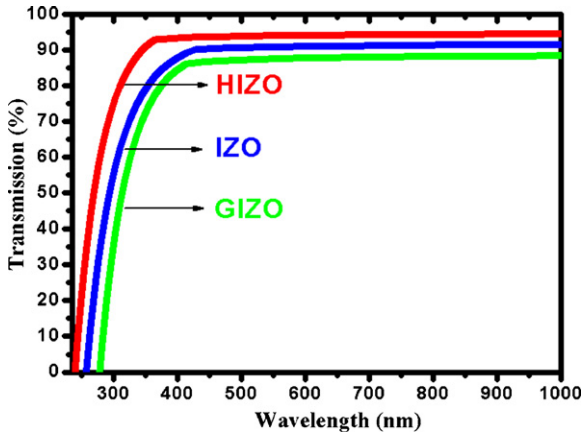

Fig. 6. Calculated data for transmission spectra as a function of wavelength for GIZO, HIZO and IZO thin films.

and μ is the absorption coefficient related to the extinction coefficient k as follows:

$$\mu = 0.82\hbar\omega k. \quad (5)$$

Here $\hbar\omega$ is the energy loss. Fig. 6 shows the optical transmission spectra as a function of the wavelength for HIZO and IZO. The transmission coefficients in the visible spectra region are approximately 87%, 90% and 94% for GIZO, IZO and HIZO, respectively. This indicates that the optical properties of IZO thin films depend on the cations incorporated into the IZO compound. The results in Fig. 6 suggest that Hf cations enhance the transmission of the IZO by 4%.

4. Conclusion

We investigated the electronic and optical properties of HIZO thin films using XPS and REELS and compared with those of GIZO and IZO thin films. XPS results showed that HIZO, GIZO, and IZO thin films have the mixed metal and oxide phases. REELS results showed that the band gap increased from 3.0 eV to 3.5 eV as a result of adding Hf to IZO. The band gaps obtained from REELS were consistent with optical band gaps determined by UV-Spectrometer. The transmission of HIZO in the visible region was enhanced in comparison to that of IZO. We attribute the increase in the transmission of HIZO to Hf cations in the HIZO thin film in comparison to that of GIZO and IZO. In conclusion, the quantitative analysis of REELS provides us with a straightforward way to determine the electronic and optical properties of transparent thin film materials.

Acknowledgment

This work was supported by the Korea Research Foundation Grant funded by the Korean Government (MOEHRD, Basic Research Promotion Fund) (KRF-2008-313-C00225).

References

[1] K. Nomura, H. Ohta, A. Takagi, T. Kamiya, M. Hirano, H. Hosono, Nature 432 (2004) 488.
[2] R.L. Hoffman, B.J. Norris, J.F. Wager, Appl. Phys. Lett. 82 (2003) 733.
[3] D. Kang, H. Lim, C. Kim, I. Song, Appl. Phys. Lett. 90 (2007) 192101.
[4] A.J. Leenheer, J.D. Perkins, M.F.A.M. van Hest, J.J. Berry, R.P. O'Hayre, D.S. Ginley, Phys. Rev. B 77 (2008) 115215.
[5] W. Lim, E.A. Douglas, S.H. Kim, D.P. Norton, S.J. Pearton, F. Ren, H. Shen, W.H. Chang, Appl. Phys. Lett. 94 (2009) 072103.
[6] J.-I. Song, J.-S. Park, H.Y.W.H. Kim, J.-H. Lee, J.-J. Kim, Appl. Phys. Lett. 90 (2007) 022106.
[7] J. Park, T. Kim, K. Son, J. Jung, K.-H. Lee, J.-Y. Kwon, B. Koo, S. Lee, IEEE Electron Device Lett. 31 (2010) 440.
[8] C.J. Kim, S. Kim, J.H. Lee, J.S. Park, S. Kim, J. Park, E. Lee, J. Lee, Y. Park, J.H. Kim, S.T. Shin, U.I. Chung, Appl. Phys. Lett. 95 (2009) 091910.
[9] S. Tougaard, F. Yubero, QUEELS-ε(k,ω)-REELS: Quantitative Analysis of Electron Energy Loss Spectra: Dielectric Function Determined by Reflection Electron Energy Loss Spectroscopy, V.3, 2008.
[10] S. Hajati, O. Romanyuk, J. Zemek, S. Tougaard, Phys. Rev. B 77 (2008) 155403.
[11] T.L. Barr, S. Seal, J. Vac. Sci. Technol. A 13 (3) (1995) 1239–1246.
[12] G.H. Kim, B.D. Ahn, H.S. Shin, W.H. Jeong, H.J. Kim, H.J. Kim, Appl. Phys. Lett. 94 (2009) 233501.
[13] D. Tahir, E.K. Lee, H.L. Kwon, S.K. Oh, H.J. Kang, S. Heo, E.H. Lee, J.G. Chung, J.C. Lee, S. Tougaard, Surf. Interface Anal. 42 (2010) 906–910.
[14] D.H. Son, D.H. Kim, J.H. Kim, S.J. Sung, E.A. Jung, J.K. Kang, Thin Solid Films 519 (2011) 6815–6819.
[15] D. Tahir, E.K. Lee, S.K. Oh, H.J. Kang, S. Heo, J.G. Chung, J.C. Lee, S. Tougaard, J. Appl. Phys. 106 (2009) 084108.
[16] F. Wooten, Optical Properties of Solid, Academic Press, New York, 1972.
[17] H. Jin, S.K. Oh, H.J. Kang, S. Tougaard, J. Appl. Phys. 100 (2006) 083713.